Insights into passive ultrasonic irrigation

Jiang, L.M.

6

Irrigant flow beyond the insertion depth of an ultrasonically oscillating file in straight and curved root canals: visualization and cleaning efficacy

Malkili M[1], Verhaagen B[2], Jiang LM[3], Nehme W[1], Naaman A[1], Versluis M[2], Wesselink PR[3], van der Sluis LW[4].

[1]Department of Endodontics, Saint-Joseph University, Beirut, Lebanon
[2]Physics of Fluids Group and MIRA Research Institute for Biomedical Technology and Technical Medicine, University of Twente, the Netherlands
[3]Department of Endodontology, Academic Centre of Dentistry Amsterdam (ACTA), University of Amsterdam and VU University, Amsterdam, The Netherlands
[4]Department of Conservative Dentistry and Endodontics, Paul Sabatier University, Toulouse, France.

Abstract

Introduction: The purposes of this study were to evaluate the influence of the insertion depth of an ultrasonically oscillating file on the ability to remove dentin debris from simulated canal irregularities in an extracted tooth model of a straight root canal and its influence on the flow of irrigant in both straight and curved canals. **Methods:** A tooth model with artificial depressions in one canal wall at 0.5, 2, 4 and 6 mm from working length was used. Ultrasonic activated irrigation was performed with the file inserted 1, 2, 3, 4 or 5 mm short of working length. Dye penetration and high-speed recordings of the flow in straight and curved canals showed the static and dynamic behavior of the flow during ultrasonic activation. **Results:** Overall cleaning efficacy decreased with increasing distance between the file and the apex, with the depressions next to the file and within 3 mm in front of the file being the cleanest. The flow observed from the visualization experiments matched this distance, suggesting a direct relation between flow and cleaning. The observed flow depth increased with increasing power setting; the curvature of the root canal had no influence on the flow depth. High-speed imaging showed a start-up phase with deeper fluid activation than in the steady phase afterwards. **Conclusion:** The ultrasonically oscillating file could remove dentin debris up to 3 mm in front of the file tip, coinciding with the extent of the observed flow. The root canal curvature had no influence on the irrigant flow.

Introduction

One of the primary goals of endodontic treatment is to heal apical periodontitis, which can be achieved by removing pulp tissue and microorganisms from the root canal system prior to placing a root canal filling (1). The complex nature of the root canal anatomy, which consists of the lumen of the main root canal(s) and accessory canals, canal ramifications, apical deltas, fins and transverse anastomoses, makes complete debridement with mechanical instrumentation alone a goal impossible to achieve (2, 3). Therefore, irrigation with a suitable disinfectant, is an essential part of a root canal treatment (4).

The apical root canal seems to be the most difficult part to clean because of its complex anatomy (5). The small dimension and complex canal structure could hinder an effective flow of the irrigant (6). Specifically, root canals often have a curvature (7), which has recently been shown to reduce the cleaning efficacy of several irrigation techniques (8, 9). Apart from the mechanical effect of removing matter (like dentin debris produced by root canal instrumentation from the apical root canal) an effective flow is needed for an adequate refreshment of the sodium hypochlorite solution (10). Unfortunately, the mechanical effect of syringe irrigation is limited in the apical root canal (5, 6). This holds also for the refreshment of the irrigant, which is shown to be limited to 1.5 mm beyond the needle tip (11). Agitation techniques could improve the apical cleaning efficacy, mechanically and chemically, by enhancing the irrigation dynamics (12).

Ultrasonic activated irrigation is one of the possibilities to agitate a sodium hypochlorite solution in the root canal (13). It has been shown that dentin debris, pulp tissue and biofilm can be removed from the root canal wall by the shear stress produced by acoustic streaming of the irrigant (14, 15). Furthermore, irrigant penetration in the apical lateral canals has been shown in an in-vitro model (16). A recent study demonstrated that dentin debris could be removed from the root canal wall 0.5 mm beyond the file tip which was positively related to the ultrasonic intensity used (17). However, it is not known how far this effect extends and how the curvature of a root canal influences this depth. Therefore, the purposes of this study were to evaluate the influence of the insertion depth of an ultrasonically oscillating file on the ability to remove dentin debris from simulated canal irregularities in an extracted tooth model of a straight root canal and its influence on the flow of irrigant in both straight and curved canals at two different ultrasonic power settings.

Materials and Methods

Dentin debris removal model
Straight roots from 15 extracted human maxillary canines were decoronated to obtain uniform root sections of 15 mm, following a previously described protocol (17). Briefly, the roots were embedded in self-curing resin (GC Ostron 100, GC Europe, Leuven, Belgium) and then bisected longitudinally through the canal in a mesiodistal direction. The surfaces of both halves were then grounded with sandpaper resulting in smooth surfaces that leave only little of the original root canal lumen. Four holes were drilled in the resin part and the two halves were reassembled by four self-tapping bolts through the holes. All the models were checked for leakage of liquid or gas apically or laterally before experiments; if there was any, rubber dam caulk would be applied to ensure that the root canal model was an entirely closed system. Standardized root canals were established by K-flexofiles #15/.02 (Dentsply Maillefer, Ballaigues, Switzerland) and GT (Dentsply, Maillefer, Switzerland) Ni-Ti rotary instruments to a working length (WL) of 15 mm, ISO size 30 and taper 0.06. Preparation was done with the final apical enlargement by the Mtwo (VDW, Munich, Germany) Ni-Ti rotary instrument #35/.04. During instrumentation, the canals were rinsed with 1 mL of 2% NaOCl after each file insertion, delivered by a 10 mL syringe (Terumo, Leuven, Belgium) and a 30-gauge needle (Navitip, Ultradent, South Jordan, UT, USA). With the help of a microscope and a round bur (H71.104.003, Komet, Lemgo Germany) attached to a drilling machine, four standard depressions (Ø=0.3 mm), located at 0.5, 2, 4 and 6 mm from WL were drilled in the wall of one half of each root canal (17). Each depression was filled with dentin debris, which was mixed with 2% NaOCl for five minutes to achieve a wet sand-like consistency, in order to simulate a situation in which dentin debris accumulates in uninstrumented canal irregularities during root canal preparation (17).

Irrigation Procedure
Specimens in all experimental groups were rinsed with 2 mL of irrigant (2% NaOCl) using 10 mL syringes with 30-gauge needles (Navitip) placed 1 mm from WL, and the flow rate was approximately 5 mL/min. Then ultrasonic activated irrigation was performed with a 21 mm, stainless steel, noncutting wire (#20, taper 00) (IrriSafe, Acteon, Merignac, France) driven by a piezoelectronic unit (Suprasson

PMax, Acteon) at power setting 'Blue 5' (frequency approximately 30 kHz, file tip displacement amplitude approximately 30 μm according to the manufacturer) for 10 seconds with the oscillation toward the depressions. The file was marked with a permanent black marker and inserted at different positions from WL, namely 1 mm from WL (group 1, n=15), 2 mm from WL (group 2, n=15), 3 mm from WL (group 3, n=15), 4 mm from WL (group 4, n=15) and 5 mm from WL (group 5, n=15). Group 6 acted as the control group, in which the ultrasonic file was inserted until 1 mm from the WL but was not activated by ultrasound. All the experimental specimens received 2 mL of irrigant, which was delivered again by syringe as final flush after the activation by ultrasound. After the irrigation, the canals were carefully dried with paper points.

Image evaluation and statistical analyses

Before and after each irrigation procedure, the root halves were separated, and the depressions were viewed through a stereomicroscope (Stemi SV6, Carl Zeiss, Göttingen, Germany) using a cold light source (KL 2500 LCD, Carl Zeiss) (17). Controls verified that no debris had fallen out of the groove during the assembly or disassembly process. Pictures were taken with a digital camera (Axio Cam, Carl Zeiss). The sequence of all the pictures was randomized. The debris removal from each depression after irrigation was scored independently and blindly by two calibrated dentists. The samples were graded as "clean" if the depression is completely clean, or "not clean" if the depression is not completely clean. The percentage of inter agreement should be more than 95%; if this percentage was lower than 95%, a consensus had to be reached. The differences in debris removal between the depressions within each group and between the groups were analyzed by Chi-square analysis. The level of significance was set at α = 0.05.

Dye penetration experiments

The depth of flow was measured statically by injecting a dye mixture (Rood, Jo-La, Bharco Foods, Baambrugge, The Netherlands; fluidic properties similar to those of water) at the coronal opening of a transparent root canal and to let it distribute by the flow generated by the ultrasonically oscillating file. Transparent root canal models were created by solidifying polydimethylsiloxane (PDMS, Sylgard 184, Dow-Corning, Midland, MI, USA) around a D-size hand spreader, leaving a root canal of size 35/.06. These silicone models have a better optical access than prefabricated Perspex blocks and allow for manufacturing of root canals with a specific curvature by pre-bending the spreader with an EndoBender (Sybron Endo, Orange, CA, USA) to create 'moderate', 'fair' or 'severe' curvatures starting at 4 or 8 mm from the tip of the spreader (WL). The exact curvatures were determined afterwards, by analyzing photos of the root canal models on the computer. A circle was drawn over the curvature, from which the radius R and the angle $α$ were obtained. From these two values, the relative arc length L^{*}_{arc} was calculated from:

$$L_{arc} = 2\pi R\, \frac{\alpha}{360}$$

$$L^{*}_{arc} = \frac{L_{arc}}{L + L_{arc}}$$

For the curvature starting at 4 mm, $L^{*}_{arc} = 0.20\pm0.02$; for the curvature starting at 8 mm, $L^{*}_{arc} = 0.35\pm0.02$. Figure 1 shows the root canal models, including analysis of their curvature. A K10/25 file was inserted to 4 or 8 mm from the apex by hand and operated for 10 seconds. Measurements were done at three power settings of the ultrasonic device (Suprasson P-Max Newtron, Acteon Satelec, Bordeaux, France), being 'Yellow 5', 'Blue 5' and 'Red 5' (in order of increasing power (17)); each measurement was performed twice. Immediately afterwards a picture was taken of the root canal with a digital camera (D5100, Nikon, Tokyo, Japan) for analysis of the depth of dye penetration.

High-speed imaging

The depth of flow was measured dynamically with the use of a high-speed camera (SA2, Photron, Tokyo, Japan), recording at 2000 frames/second to record the movement of microparticles inside a transparent root canal model (14). The same models as in the dye penetration study were used. The K10/25 file was inserted to 4 or 8 mm from the apex and centered laterally in the canal. The root canal was then filled with water, to which hollow glass spheres with a diameter of 10 μm were added as tracer particles. The root canal was fitted in front of a microscope (BX-FM, Olympus, Tokyo, Japan) with $2.5\times$ magnification; light was provided in bright-field mode using a continuous cold-light source (ILP-1, Olympus). Measurements were done at the three power settings also used in the dye penetration experiments. Analysis of the recordings was performed by subtracting consecutive frames in the recordings; a movement of the microparticles resulting from the induced flow leads to a change

between the two image frames and therefore gives an indication of the image areas where flow was present.

Results

The results are presented in figure 2. The ultrasonically activated groups removed more dentin debris than the non activated control group (P < 0.0001). Group 1 and 2, with the file positioned 1 and 2 mm from WL, exhibited significantly better cleaning efficacy than the other groups, followed by group 3 which removed significantly more debris than group 4 and 5. There was no significant difference between the four levels of the depression in groups 1 and 2, in contrast to groups 3, 4 and 5. Cleaning was observed up to 3 mm apically from the file tip with no significant difference between 0.5 and 2mm from the tip. The Kappa value was 0.85.

The dynamical behavior of the flow, during the first 200 milliseconds after start-up, is shown in figure 3, where the relative amount of flow is plotted as a function of depth and time. The graph shows a start-up phase with deeper fluid activation than in the steady phase afterwards. The final state (flow depth beyond the file tip) for each power setting and curvature, as obtained with the dye penetration experiments, is shown in figure 4. For power setting 'Yellow 5' the flow depth is typically slightly more than half of the distance to the apex; increasing the power setting increased the flow depth. At 'Blue 5' and an insertion depth of 4 mm from the apex of a straight canal, the flow depth was approximately 3 mm, in agreement with the cleaned areas in the extracted tooth experiments. The curvature did not have a significant influence on the flow depth.

Discussion

In ultrasonically activated irrigation, the irrigant is activated corresponding to a characteristic pattern of nodes and antinodes along the oscillating file (18). The induced acoustic streaming leads to jets of irrigant that are directed towards the root canal wall (17). These jets are responsible for the removal of dentin debris from artificial holes in the root canal wall (lateral cleaning effect of the ultrasonically oscillating file) (14). This cleaning effect can be observed from the coronal to the apical part of the root canal (17, 19). Previous work reported a cleaning effect even 0.5 mm beyond the file tip which increased with increasing intensity of the ultrasonic power (17).

In this study we demonstrated that in straight canals this cleaning effect extends until 3 mm in front of the file tip (power setting 'Blue 5', distance file tip-apex 4 mm), and that the cleaning effect decreases with the distance of the file tip to the depression filled with dentin debris (Figure 2). We observed by visual methods that the flow depth of the irrigant is also 3 mm (at the same power setting and distance file tip-apex), suggesting a direct relation between flow and cleaning. The transparent root canal model therefore gives some insight into the irrigant dynamics responsible for cleaning. However, the exact relation between flow and cleaning efficacy needs further studying, as the more complex geometry (including the artificial depressions) of the root canal in the extracted teeth will affect the flow compared to the smooth transparent root canal model. There could also be a difference in the reflection of ultrasound by the silicon (transparent) root canal model walls compared to dentinal walls; however the high-speed imaging showed no deformation of the silicone walls, therefore it was assumed that the silicone walls acted as solid walls for the fluid flow.

For syringe irrigation, only severe root canal curvatures influence the cleaning efficacy (20). However, in ultrasonically activated irrigation the irrigant penetration is only influenced by the ultrasonic intensity (17) and the distance file tip-apex, if the file is placed without constraint in a curved root canal (just before the curve). The observation that the curvature doesn't influence the flow depth, see Figure 4, suggests that the microstreaming occurs typically on a much smaller scale than the curvature. Therefore, the apical extent of cleaning in curved canals will be comparable to the apical extent of cleaning in straight canals. It also suggests that origin of the limitation in reaching the apex in a curved canal is not of fluid dynamical nature but is rather related to geometrical aspects, such as the location and length of the curvature. There is a difficulty in bringing the file tip close to the apex, which requires (pre)-bending of the file and/or implies much forced contact with the root canal wall, which both may alter the file oscillation significantly, reduce the efficacy of the irrigant streaming and increase the risk on file fracture. This is typically the case in the study of Amato (21), were the curvature was at 7 mm from the apex and the file placed 1 mm short of working length. In the study of Rodig (19), apart from the curvature and the placement of the file 2 mm from working length, a cutting K-file instead of a non-cutting file and the activation time (two times 1 minute) could have resulted in the production of dentin debris and explain that they did not find a significant difference between

(ultra)sonic activation of the irrigant or no activation (19). The ultrasonic intensity for both studies was low.

In this study we have considered the influence of the curvature of the root canal on the flow. It is known that for syringe irrigation the size and taper of the root canal have an influence on the irrigant flow (6, 22). For ultrasonic activation of an irrigant, an increasing taper influences positively the removal of dentin debris from the root canal when the irrigant is applied continuously in the pulp chamber (23). However in this study, the irrigant was delivered in the root canal by a syringe and then activated by an ultrasonically oscillating file. If we only evaluate the individual depressions, it is interesting to notice that the cleaning efficacy from these depressions is very similar, but the dimension of the root canal actually changed from apical to the coronal, from 0.39 mm (1 mm from WL) to 0.60 mm (5 mm from WL). According to this result, we could conclude that within this range, the dimension of the root canal did not influence the efficacy of dentin debris removal of the ultrasonic activation of the irrigant, which was delivered by a syringe in the root canal.

The conclusion we can draw from the current study is that the ultrasonically oscillating file could remove dentin debris from the root canal wall up to 3 mm in front of the file tip, coinciding with the observed flow. Furthermore, the root canal curvature had no influence on the irrigant flow.

Figure 1. Overview of the curved transparent root canal models. The curvature is varied from 'none' (a,e) to 'moderate' (b,f), 'fair' (c,g) to 'severe' (d,h); the curvature starts at 4 mm (a-d; $L* = 0.20$) or 8 mm (e-h; $L* = 0.35$) from the apex.
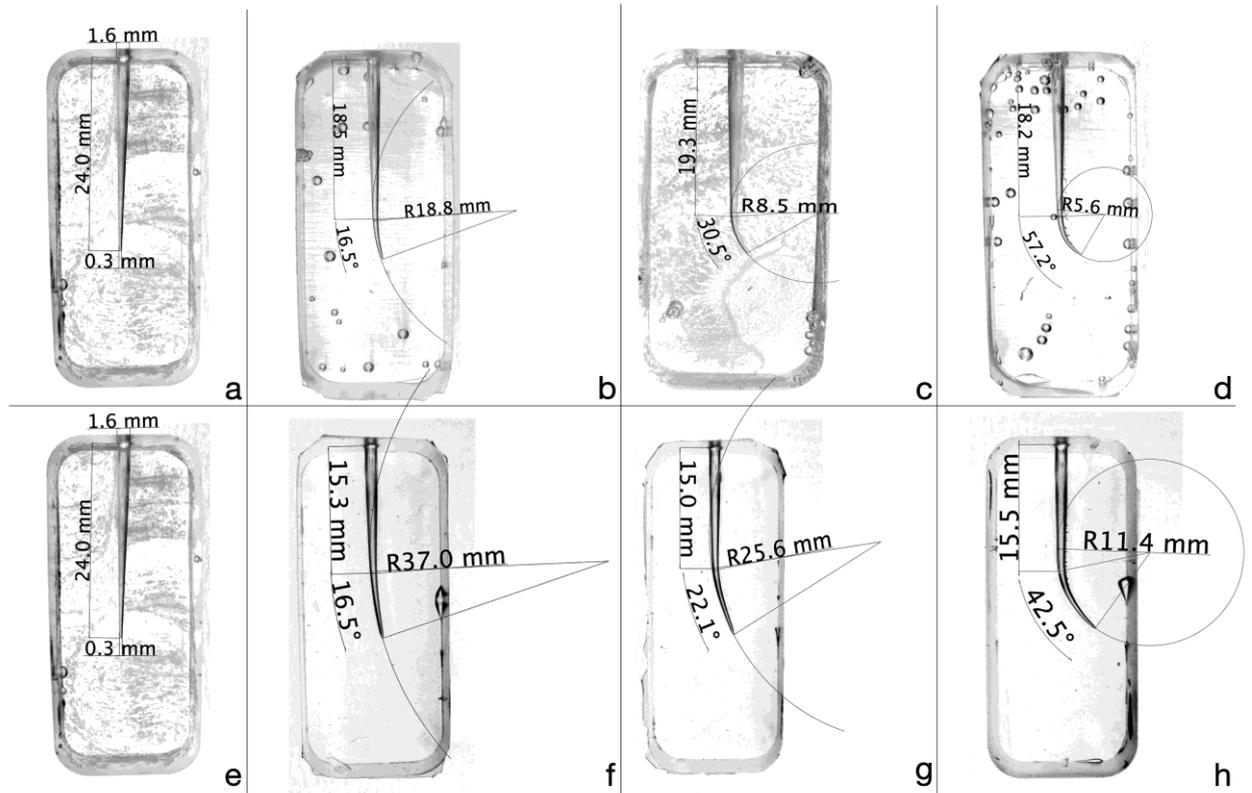
Figure 2. The percentage of completely clean depressions after the irrigation procedure in each experimental group
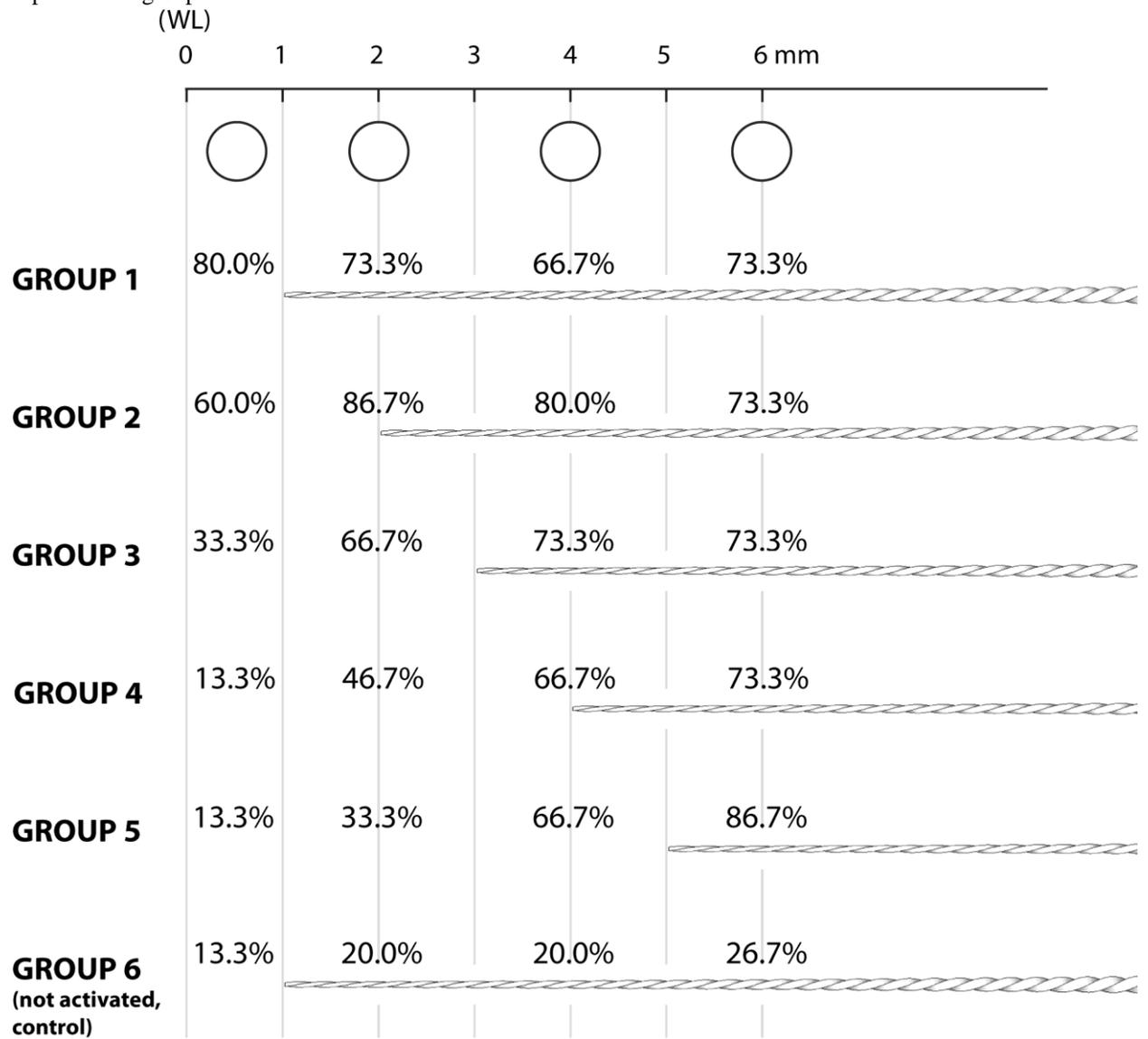
Figure 3. Flow depth as a function of time for the first 200 milliseconds after start of the file oscillation. The left panel shows the initial state (note the different scales on the x- and y axis); the right panel shows the flow depth (y-axis, same scale as the left panel) over time (x-axis). Colors represent change between frames, representing flow. Power setting is 'Yellow 5', distance file tip to apex is 4 mm; moderate curvature.
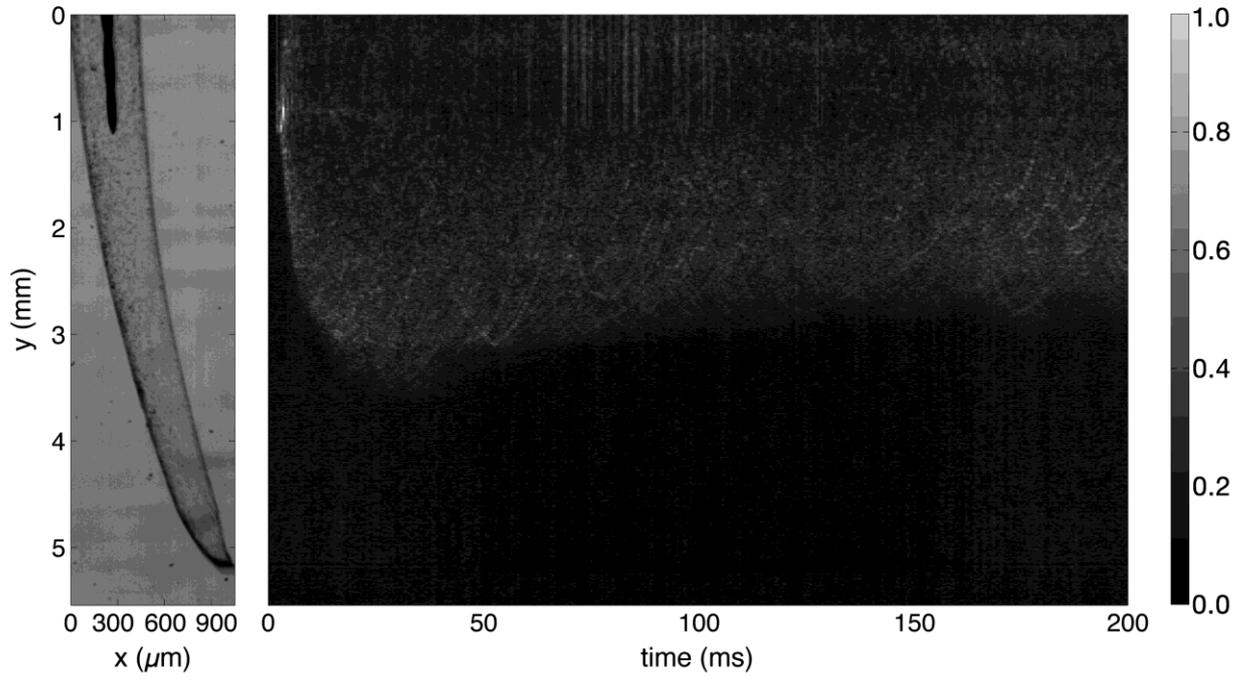
Figure 4. Flow depth beyond the file as a function of curvature and power setting (represented by line color, with red > blue > yellow). The y-axis labels show the flow depth beyond the file in millimeter (left) and in percentage of the distance between file tip and apex (right). *L** is the relative size of the curvature, which is also the relative distance from the apex where the file was positioned.
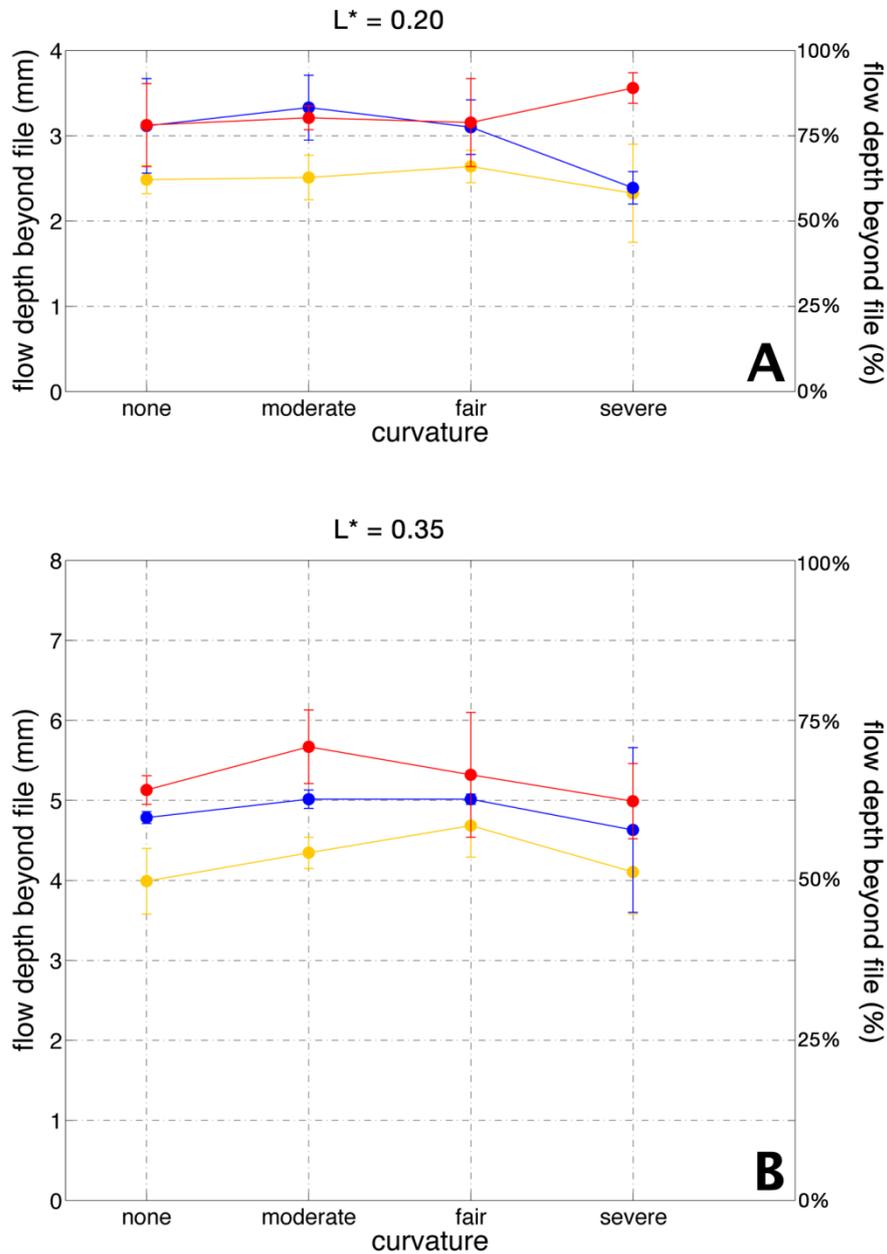
References

1. Siqueira JF, Rôças IN. Clinical implications and microbiology of bacterial persistence after treatment procedures. J Endod 2008;34,1291–301.
2. Baker NA, Eleazer PD, Averbach RE. Scanning electron microscopic study of the efficacy of various irrigating solutions. J Endod 1975;1,127–35.
3. Siqueira JF, Lima DC, Magalhaes FAC, et al. Mechanical reduction of the bacterial population in the root canal by three instrumentation techniques. J Endod 1999;25:332–5.
4. Gulabivala K, Patel B, Evans G, Ng YL. Effects of mechanical and chemical procedures on root canal surfaces. Endod Topics 2005;10,103–22.
5. Naïr PNR, Henry S, Cano V, et al. Microbial status of apical root canal system of human mandibular first molars with primary apical periodontitis after 'one visit' endodontic treatment. Oral Surg, Oral Med Oral Pathol Oral Radiol Endod 2005;99,231-52.
6. Boutsioukis C, Verhaagen B, Kastrinakis E, et al. The effect of preparation size on the irrigant flow in the root canal: evaluation using an unsteady Computational Fluid Dynamics model. Int Endod J 2010;43,874-81.
7. Cunningham C, Senia E. A 3-Dimensional study of canal curvatures in the mesial roots of mandibular molars. J Endod 1992;18,294–300.
8. Amato M, Vanoni-Heineken I, Hecker H, Weiger R. Curved versus straight root canals: the benefit of activated irrigation techniques on dentin debris removal. Oral Surg, Oral Med Oral Pathol Oral Radiol Endod 2011;111,529–534.
9. Rödig T, Döllmann S, Konietschke F, et al. Effectiveness of different irrigant agitation techniques on debris and smear layer removal in curved canals: a scanning electron microscopy study. J Endod 2010;36,1983-7.
10. Haapasalo M, Endal U, Zandi H et al. Eradication of endodontic infection by instrumentation and irrigation solutions. Endod Topics 2005;10,77-102.
11. Boutsioukis C, Verhaagen B, Kastrinakis E, Versluis M, van der Sluis LW. Evaluation of irrigant flow in the root canal using different needle types by an unsteady Computational Fluid Dynamics model. J Endod 2010;36,865-9.
12. Gu LS, Kim JR, Ling J, et al. Review of contemporary irrigation and agitation techniques and devices. J Endod 2009;35,791-804.
13. Lee SJ, Wu MK, Wesselink PR. The effectiveness of syringe irrigation and ultrasonics to remove debris from simulated irregularities within prepared root canal walls. Int Endod J 2004;37:672–8.
14. Jiang LM, Verhaagen B, Versluis M, van der Sluis LWM. The influence of the orientation of an ultrasonic file on the cleaning efficacy of ultrasonic activated irrigation. J Endod 2010;36,1372-6.
15. Burleson A, Nusstein J, Reader A, Beck M. The in vivo evaluation of hand/rotary/ultrasound instrumentation in necrotic human mandibular molars. J Endod 2007;33,782-7.
16. de Gregorio C, Estevez R, Cisneros R, et al. Effect of EDTA, sonic and ultrasonic activation on the penetration of sodium hypochlorite into simulated lateral canals: an in vitro study. J Endod 2009;35,891-5.
17. Jiang LM, Verhaagen B, Versluis M, et al. The influence of the ultrasonic intensity file on the cleaning efficacy of passive ultrasonic irrigation. J Endod 2011;37,688-92.
18. Ahmad M, Pitt Ford TR, Crum LA. Ultrasonic debridement of root canals: an insight into the mechanisms involved. J Endod 1987;13,93-101.
19. Rödig T, Bozkurt M, Hulsmann M. Comparison of the vibringe system with syringe and passive ultrasonic irrigation in removing debris from simulated root canal irregularities. J Endod 2010;36,1410-13.
20. Nguy D, Sedgley C. The influence of canal curvature on the mechanical efficacy of root canal irrigation in vitro using real-time imaging of bioluminescent bacteria. J Endod 2006;32,1077-80.
21. Amato M, Vanoni-Heineken I, Hecker H, Weiger R. Curved versus straight root canals: the benefit of activated irrigation techniques on dentin debris removal. Oral Surg, Oral Med Oral Pathol Oral Radiol Endod 2011;111,529–534.
22. Boutsioukis C, Verhaagen B, Kastrinakis E, Versluis M, van der Sluis LWM. The effect of root canal taper on the irrigant flow: evaluation using an unsteady Computational Fluid. Int Endod J 2010;43,909-16.
23. van der Sluis LWM, Wu MK, Wesselink PR. The efficacy of ultrasonic irrigation to remove artificially placed dentine debris from human root canals prepared using instruments of varying taper. Int Endod J. 2005;38,764-8..